J. R. Gordon and S. J. Garwood†*

Ductile Fracture in Aluminium Alloy Weldments

REFERENCE Gordon, J. R. and Garwood, S. J., **Ductile fracture in aluminium alloy weldments**, *Defect Assessment in Components – Fundamentals and Applications*, ESIS/EGF9 (Edited by J. G. Blauel and K.-H. Schwalbe) 1991, Mechanical Engineering Publications, London, pp. 925–940.

ABSTRACT This paper presents the results of a large test programme undertaken to study ductile fracture in aluminium weldments. The main body of the experimental programme consisted of a series of wide plate tests on 50 mm thick welded aluminium alloy panels. In addition to the wide plate tests, tensile, and single specimen unloading compliance R curve tests were conducted on specimens extracted from the various test panels. The through-thickness residual stress distributions in the welded panels were measured experimentally so that the influence of residual stresses on ductile fracture could be assessed.

The wide plate tests were analysed using a CTOD strip yield model, and reference stress model. It was found that tearing instability assessments performed using the CTOD reference stress model provided conservative but reasonable accurate predictions of maximum far field stress, provided residual stresses were included in the analysis and the CTOD R curve was obtained from full thickness sidegrooved single edge notch bend (SENB) fracture toughness specimens.

Introduction

In a ductile fracture assessment the resistance curve for the material is compared against a series of driving force curves. The principle behind this analysis is shown schematically in Fig. 1. In this diagram the material's CTOD R curve is represented by the solid curve denoted δ_R. The R curve is positioned so that it intersects the crack length axis at a value corresponding to the initial crack length in the structure, a_0.

The maximum load carrying capacity of the structure is defined by P_2, where the driving force curve is tangential to the R curve, i.e., point C. This condition can be expressed mathematically as

$$\delta_A = \delta_R \text{ and } \frac{d\delta_A}{da} = \frac{d\delta_R}{da} \tag{1}$$

This paper presents the results of four wide plate and associated small scale fracture tests on 50 mm thick welded aluminium panels. The results obtained from wide plate and small scale fracture tests on 10 mm thick welded aluminium panels have been reported previously **(1)**. All the test panels were supplied by Alcoa Technical Centre. The tests are analysed using CTOD strip

* Edison Welding Institute, 1100 Kinnear Road, Columbo, Ohio 43212, USA.
† The Welding Institute, Abington, Cambridge, CB1 6AL, UK.

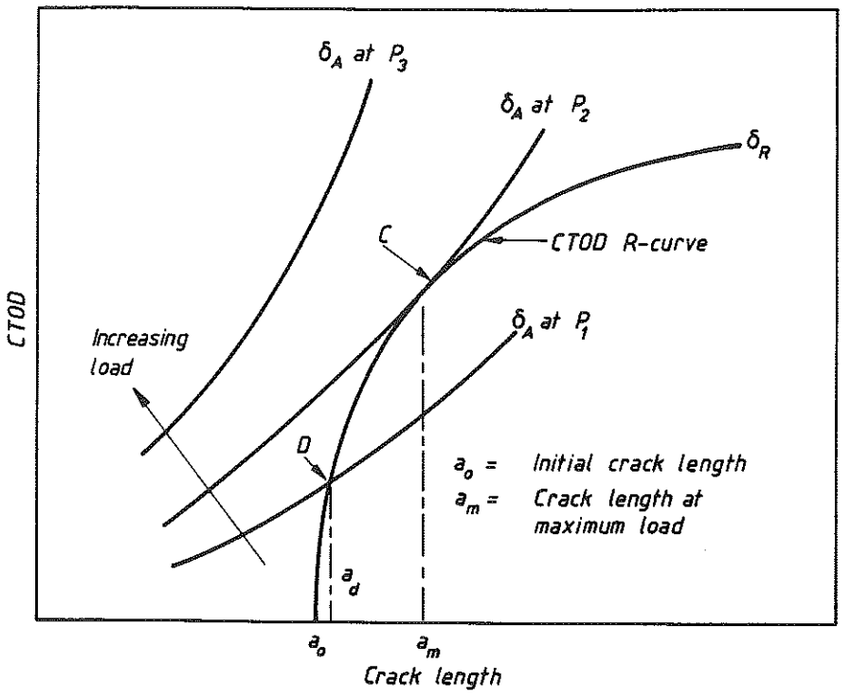

Fig 1 Principle of *R* curve analysis

yield **(2)** and reference stress models **(3)**. The predicted and actual conditions at maximum load are compared.

Fracture assessment models

General

The collapse modified strip yield and reference stress fracture assessment models compared in this paper are expressed as functions of effective primary stress σ_p, effective secondary stress σ_s and effective net section stress σ_n **(4)**. The effective primary and secondary stress terms are given by the following expressions where K_I^p and K_I^s are the stress intensity factors due to primary and secondary stresses respectively

$$\sigma_p = \frac{K_I^p}{\sqrt{(\pi a)}} \quad \sigma_s = \frac{K_I^s}{\sqrt{(\pi a)}} \tag{2}$$

The dimension a corresponds to the flaw dimension of interest, i.e., the half length of a through-thickness flaw, the depth of a surface flaw, or the half height of an embedded flaw. The effective primary and secondary stresses have the units of stress but, in general, are not equal to the actual primary and

secondary stresses. (The exception is an infinite plate in uniform tension with a through thickness flaw of length $2a$). The effective primary and secondary stresses are simply convenient parameters that contain the stress intensity and flaw size.

The effective net section stress, σ_n, characterises the primary stress in the uncracked area of the section under consideration. Net section yield occurs when σ_n is equal to the yield stress.

Plastic collapse modified strip yield model

The CTOD plastic collapse modified strip yield fracture assessment model employed in this investigation **(1)** can be expressed as

$$\delta = \frac{\sigma_{YS}\pi a}{E}\left[\left(\frac{\sigma_p+\sigma_s}{\sigma_{YS}}\right)^2 + \frac{1}{2}\left(\frac{\sigma_s}{\sigma_{YS}}\right)^4 + \left(\frac{\sigma_p}{\sigma_{YS}}\right)^2 \times \left\{\left(\frac{\sigma_{flow}}{\sigma_n}\right)^2 \frac{8}{\pi^2} \ln \sec\left(\frac{\pi}{2}\frac{\sigma_n}{\sigma_{flow}}\right) - 1\right\}\right] \tag{5}$$

where

σ_{YS} = yield strength
σ_{flow} = flow strength given by $\sigma_{flow} = (\sigma_{YS} + \sigma_{TS})/2$
σ_{TS} = tensile strength
E = Young's modulus

In the above expression the total applied CTOD is made up of:

(i) an elastic component based on primary and secondary stresses;
(ii) a first order plastic zone correction term based on secondary stresses;
(iii) a plastic component based on primary stresses, which is assumed implicitly to include a first order plastic zone correction for primary stresses.

Reference stress model

The CTOD reference stress fracture assessment model is given by **(1)**

$$\delta = \frac{\pi\sigma_{YS}^a}{E}\left\{\left(\frac{\sigma_p+\sigma_s}{\sigma_{YS}}\right)^2\left(\frac{E}{E'}\frac{a_e}{m_{el}a}\right) + \left(\frac{\sigma_p}{\sigma_{YS}}\right)^2 \frac{\mu}{m_{FP}}\left(\frac{E\varepsilon_{ref}}{\sigma_{ref}} - 1\right)\right\} \tag{6}$$

where a_e is given by

$$a_e = a + \frac{1}{\beta\pi}\frac{n-1}{n+1}\frac{(\sigma_p+\sigma_s)^2\pi a}{\sigma_{YS}^2}\frac{1}{1+(\sigma_{ref}/\sigma_{YS})^2} \tag{7}$$

and

m_{el} = 1 for plane stress and $m_{el} = 2$ for plane strain
m_{FP} = 1.1 for tension and $m_{FP} \simeq 1.3$–1.8 for bending
μ = 0.75 for plane stress and $\mu = 1.0$ for plane strain
E' = E for plane stress and $E' =$ for $E/(1-\nu^2)$ for plane strain
β = 2 for plane stress and $\beta = 6$ for plane strain.

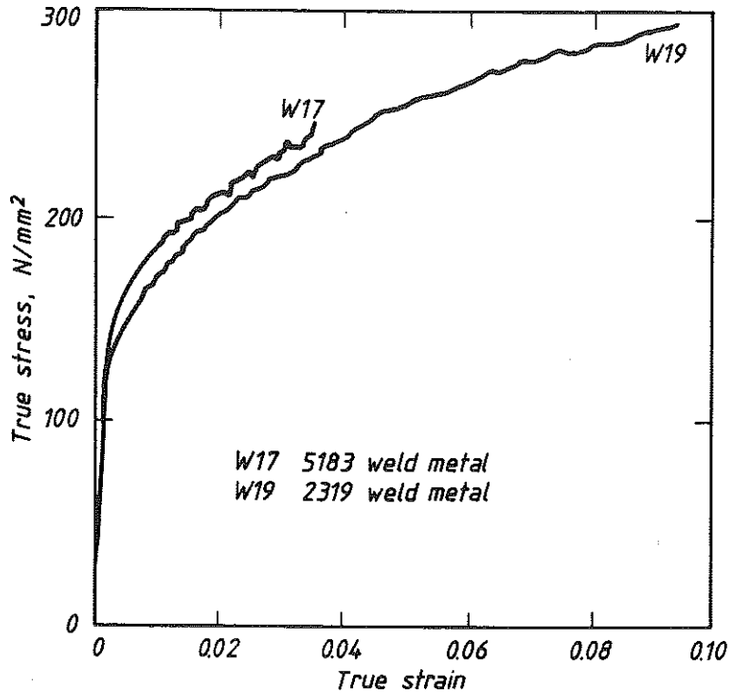

Fig 2 True stress–true stress curves for 5183 and 2319 aluminium alloy weld metals

The reference stress, (σ_{ref}) in equations (6) and (7) is equal to the effective net section stress. The reference strain (ε_{ref}), is defined as the value of strain corresponding to σ_{ref} in a uniaxial tensile test.

In the CTOD reference stress equation, the total applied CTOD is made up of:

(i) an elastic component (which includes a first order plastic zone correction) based on primary and secondary stresses;
(ii) a fully plastic component based on primary stresses.

Details of the collapse modified strip yield and reference stress fracture assessment models are given in reference **(1)**. Expressions for calculating the effective net section stress (σ_n) for a range of crack geometries are presented in reference **(5)**.

Details of aluminium alloy test panels

A total of four wide plate tests were conducted in this investigation, on 50 mm thick aluminium alloy welded panels supplied by Alcoa Technical Centre. The welded panels, which contained double 'V' butt welds, were fabricated in pairs

Table 1 Details of test panel materials

Panels	*Parent metal*	*Welding consumable*
W17, W18	5083-0	5183
W19, W20	2219-T87	2319

Alloy designations to ASTM-B209

Chemical composition of plate material and welding wires (wt%)

Description	*Si*	*Fe*	*Cu*	*Mn*	*Mg*	*Cr*	*Zn*	*Ti*	*V*	*Zr*
5083-0 plate	0.10	0.28	0.04	0.65	4.36	0.11	0.04	0.03	0.01	0.00
2219-T87 plate	0.07	0.21	6.15	0.23	0.01	0.00	0.05	0.06	0.10	0.12
5183 wire	0.09	0.16	0.01	0.58	4.52	0.06	0.04	0.07	0.01	0.00
2319 wire	0.10	0.17	6.35	0.27	0.01	0.00	0.03	0.14	0.10	0.12

Data supplied by Alcoa

using the MIG process. Details of the parent plate/weld combinations of the panels are given in Table 1.

Details of test programme

Tensile tests

The true stress–true strain behaviour of the two aluminium alloy weld metals was determined by testing flat cross weld tensile specimens with high elongation strain gauges attached to the weld (one on each side of the specimen). Before strain gauging the specimens, the weld overfill was machined off flush with the surface of the parent plate. The true stress–true strain curves of the two weld metals are compared in Fig. 2 whilst the tensile properties are summarised in Table 2.

Table 2 Tensile properties of parent plate and weld metals

			Parent metal		*Weld metal (all weld metal specimens)*	
Testplates	*Parent metal*	*Weld metal*	*0.2% proof strength, (N/mm^2)*	*Tensile strength, (N/mm^2)*	*0.2% proof strength, (N/mm^2)*	*Tensile strength, (N/mm^2)*
W17, W18	5083-0	5183	136	301	159	301
W19, W20	2219-T87	2319	356	446	130	274

Ramberg–Osgood stress–strain constants (interpreted from Fig. 2)

Materials	*Panels*	*Weld metal*	σ_o, (N/mm^2)	ε_o	α	η
5083/5183	W17, W18	5183	159	0.00227	1.21	6.39
2219/2319	W19, W20	2319	130	0.00186	1.15	5.16

$$\frac{\varepsilon}{\varepsilon_o} = \frac{\sigma}{\sigma_o} + \alpha\left(\frac{\sigma}{\sigma_o}\right)^{\eta}$$

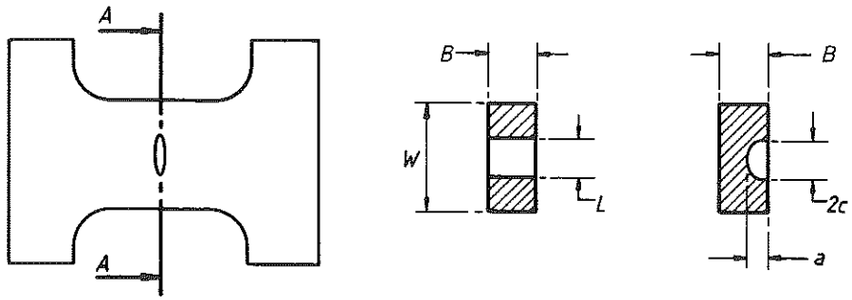

Material	Wide plate	W	L/2	a	2c	B
5083/5183	W17	450	31.9	—	—	47
5083/5183	W18	450	—	18.2	101.5	48
2219/2319	W19	442	28.3	—	—	51
2219/2319	W20	450	—	14.6	104.6	51

Fig 3 Details of wide plate specimens

Wide plate tests

Details of the centre cracked panel (CCP) and semi-elliptical surface notched tension (SESNT) wide plate specimens are summarised in Fig. 3. The welded specimens were notched in the weld metal with the weld axis at right angles to the loading direction of the plate. All the wide plate specimens were fatigue pre-cracked in cyclic tension prior to testing.

The wide plate specimens were loaded in displacement control. During the tests the applied load, four clip gauges and two long range displacement transducers were continually monitored by a computerised data acquisition system.

Small scale fracture toughness tests

Small scale single edge notch bend (SENB) fracture toughness specimens were extracted from all four welded test panels to enable the crack growth resistance behaviour of the two weld metals to be determined. The small scale tests were performed on both surface and through thickness notched specimens as illustrated in Fig. 4.

The surface notched specimens were square in cross section, i.e., B × B, whereas the through thickness specimens were rectangular in cross section, i.e., B × 2B. All the specimens were nominally full plate thickness and were notched at the weld centreline.

Before the SENB specimens were fatigue pre-cracked they were mechanically stress relieved by compressing the ligament in front of the machined

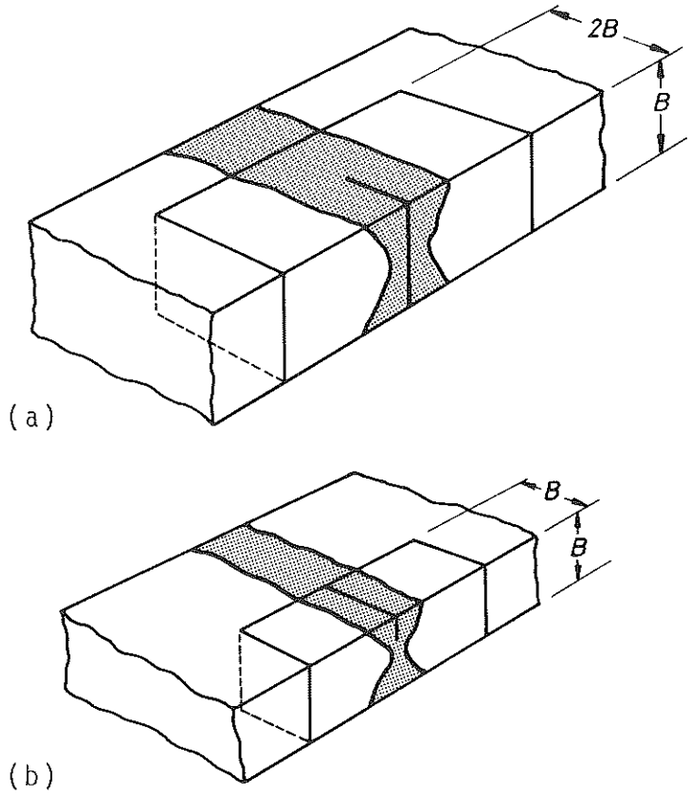

Fig 4 Typical examples of specimen extraction associated with standard specimen designs
(a) Through-thickness notch
(b) Surface notch

notch to produce a plastic strain of approximately 1 percent of the specimen thickness. Previous work at The Welding Institute **(6)** has indicated that local compression reduced the transverse residual stresses significantly and results in improved fatigue crack shapes. Following the local compression operation the SENB specimens were fatigue pre-cracked to provide initial crack depth to specimen width ratios of approximately 0.5. The specimens were then tested at room temperature using unloading compliance procedures to produce CTOD R curves. It should be noted that although the local compression will have reduced the transverse residual stresses in the small scale SENB specimens significantly, residual stresses will still undoubtedly have been present in these specimens prior to testing.

The small scale tests were performed in groups of three. One specimen in each group was sidegrooved by 20 percent, whilst the remaining two specimens in each group were tested in the plane sided configuration.

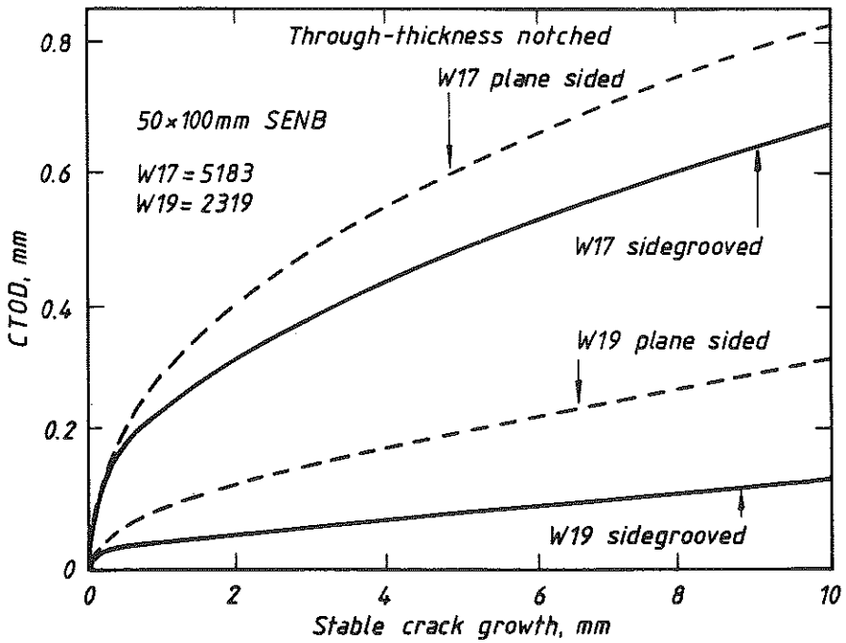

Fig 5 Sidegrooved and plane sided SENB CTOD *R* curves for welds W17 (5183) and W19 (2319) (through-thickness notched specimens)

The small scale CTOD R curves obtained from the through thickness and surface notched specimens are presented in Fig. 5 and 6 respectively. As expected the CTOD R curves obtained from the sidegrooved specimens are in general, slightly lower than the R curves obtained from the corresponding plane sided specimens. Although machining the sidegrooves in the small scale SENB specimens will probably have caused minor relaxation in the transverse residual stresses the difference in R curve behaviour of the plane sided and sidegrooved specimens is considered to be a result of the additional constraint provided by the sidegrooves.

Residual stress measurements

Residual stresses form in welded joints as a result of the thermal cycle which accompanies the welding process. Typical longitudinal and transverse residual stress distributions associated with a double 'V' butt weld are presented schematically in Fig. 7. To enable the significance of residual stresses on ductile fracture to be assessed the transverse residual stress distributions in the welded aluminium panels were measured experimentally.

The through-thickness distributions of the transverse residual stresses in panels W17 and W19 were determined using a two stage sectioning technique

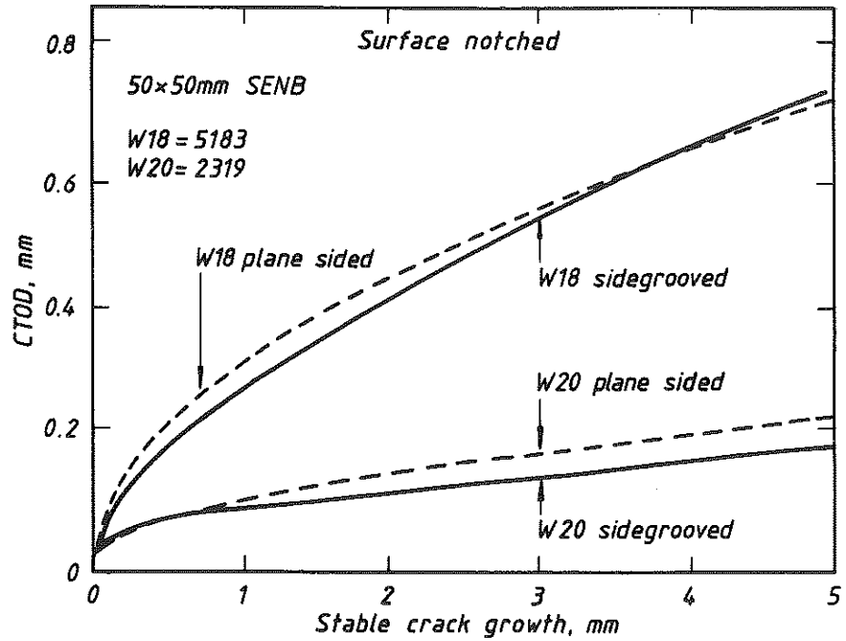

Fig 6 Sidegrooved and plane sided SENB CTOD *R* curves for welds W18 (5183) and W20 (2319) (surface notched specimens)

(7). The typical experimental error associated with block removal and layering procedures is estimated to be ± 10 N/mm^2 **(8)** for ferritic steels. As a result of the difference in Young's modulus of aluminium and steel the accuracy of the sectioning technique should be improved for aluminium welded joints.

The transverse residual stress distributions measured at the weld centreline in panels W17 and W19 are plotted in Figs 8 and 9.

Comparison of fracture assessment models

General

Tearing instability assessments were undertaken on the four welded wide plate tests. To examine whether residual stresses have a significant effect on tearing instability analyses of cracks in fully ductile metals, the fracture assessments were performed both including and ignoring the residual stresses induced by welding. For the centre cracked panels (i.e., wide plates W17 and W19) the values of residual stress included in the strip yield and reference stress models corresponded to the maximum measured transverse residual stress on the weld centreline in the appropriate test panel. In the case of the surface notched wide plate specimens (i.e., wide plates W18 and W20) the strip yield and reference

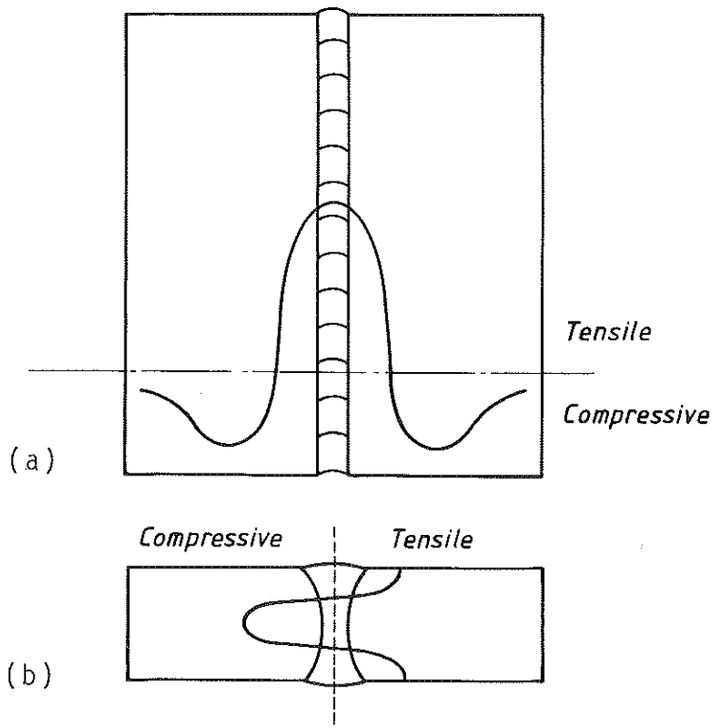

Fig 7 Typical residual stress distributions associated with a double 'V' butt weld
(a) Longitudinal residual stress distribution
(b) Through-thickness distribution of transverse residual stresses

stress fracture assessments were conducted with an assumed linear residual stress distribution which was greater than the measured residual stress distribution over the defect depth. Moreover, the assumed residual stress distribution was adjusted so that up to approximately 5 mm of stable crack growth could be tolerated before the measured transverse residual stress exceeded the assumed value. The assumed transverse residual stress distributions for the strip yield and reference stress model assessments of panels W18 and W20 are compared with the measured distributions obtained from panels W17 and W19 in Figs 8 and 9.

Tearing instability assessments

Driving force/R curve tearing instability analyses were conducted for each wide plate specimen, by comparing the CTOD R curves obtained from the small scale specimen tests against computer generated driving force curves calculated using the collapse modified strip yield and reference stress models. Assessments were performed both including and ignoring residual stresses.

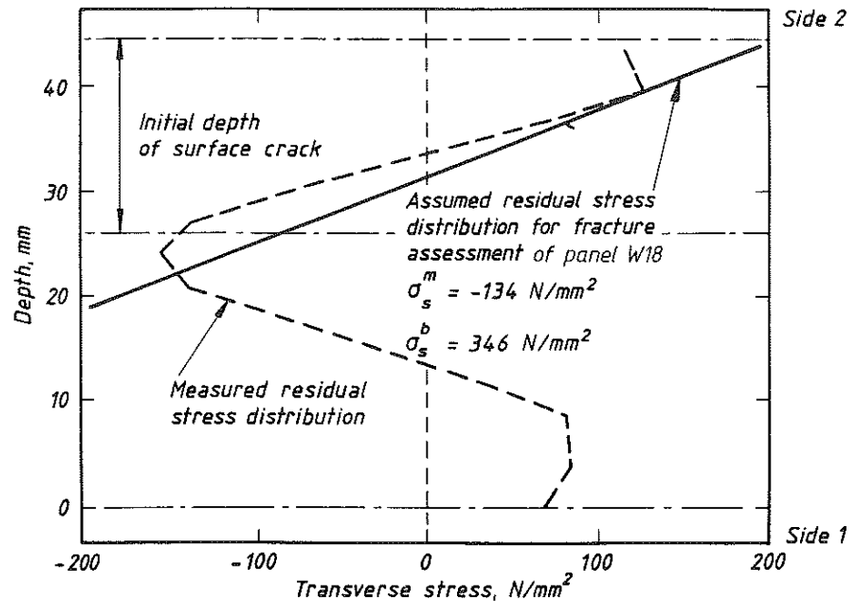

Fig 8 Comparison of measured transverse residual stress distribution in panel W17 (5183) and residual stress distribution assumed in fracture assessment of panel W18 (5183)

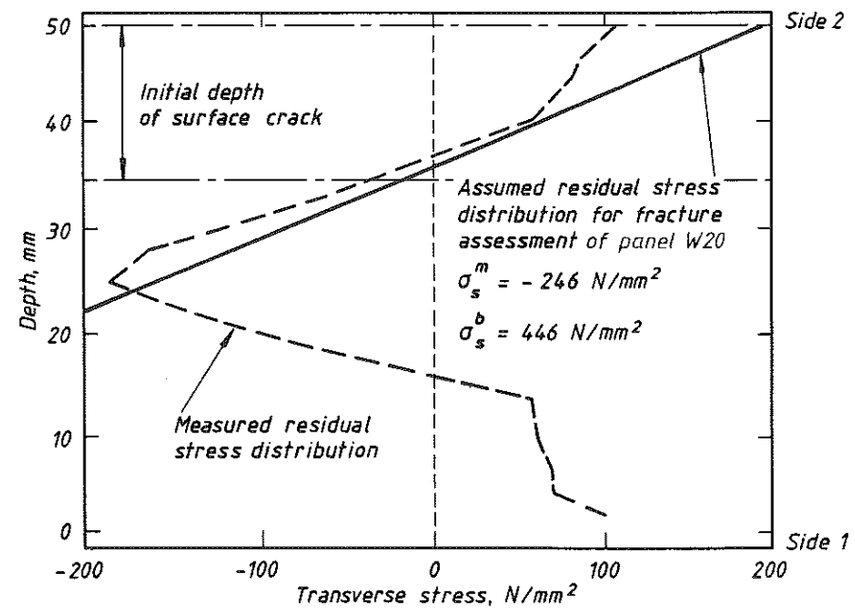

Fig 9 Comparison of measured panel W19 (2319) and residual stress distribution assumed in fracture assessment of panel W20 (2319)

Moreover, assessments were performed using both the CTOD R curve obtained from the sidegrooved SENB specimen from the appropriate set of small scale fracture toughness specimens and the mean CTOD R curve obtained from the remaining two plane sided specimens from the same set.

The reference stress model requires stress–strain information of the parent material/weld metal under consideration. In this investigation the assessments based on the reference stress model were conducted using the actual true stress–true strain behaviour of the appropriate weld metal. Moreover, since the nominal thickness of the wide plate specimens was 50 mm, the reference stress model assessments were performed assuming a state of plane strain.

It should be emphasised that, even if elastic–plastic plane strain thickness requirements are satisfied, the slope of an R curve is dependent on the geometry of the specimen and in particular the mode of loading. The lowest R curves are produced by specimens which experience a large bending component. Consequently it is normal practice to employ R curves obtained from laboratory type bend specimens (e.g., SENB or compact) in ductile structural integrity assessments to increase the degree of conservatism.

For this reason the tearing instability assessments undertaken for the four wide plate specimens should predict values of maximum far field stress which are lower than the actual values observed in the tests.

The results of the tearing instability analyses are summarised in Figs 10–13. Figures 10 and 11 show the effect of incorporating CTOD R curves from plane

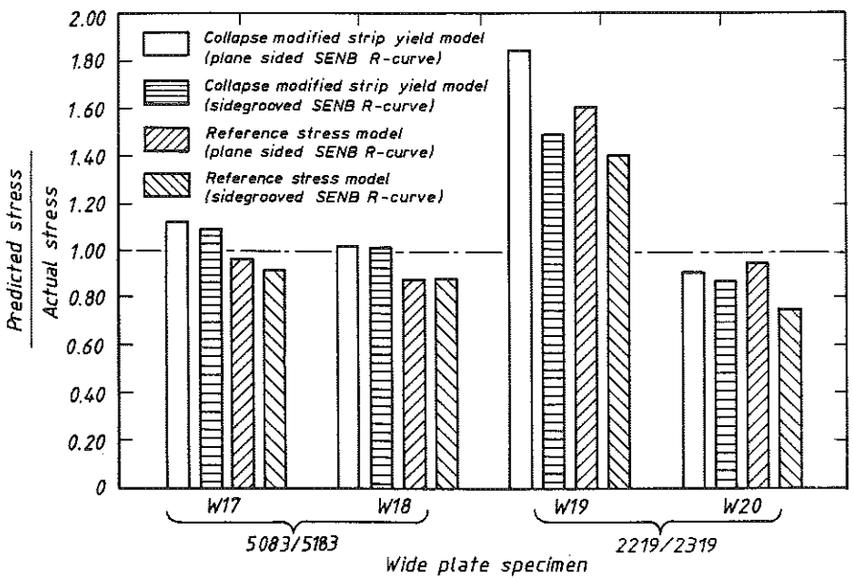

Fig 10 Comparison of tearing instability assessments (residual stresses not included in analysis

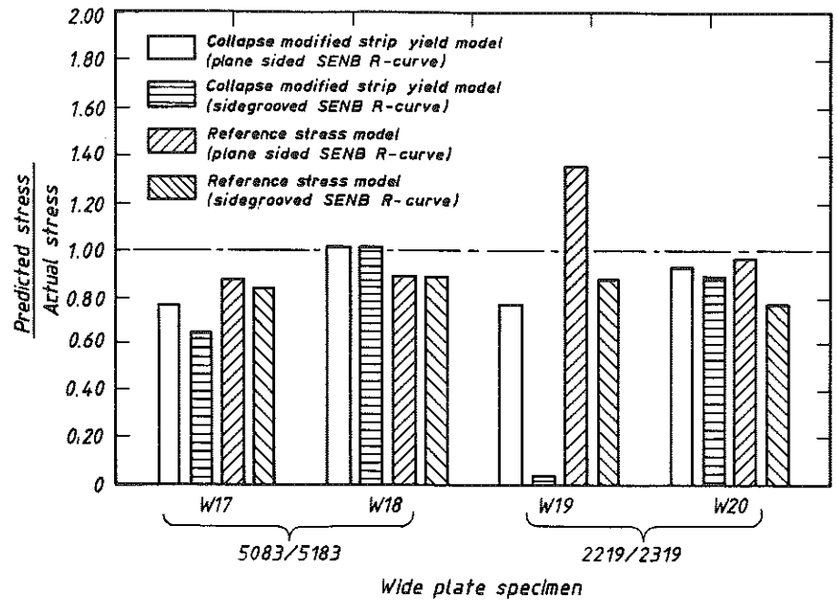

Fig 11 Comparison of tearing instability assessments (residual stresses included in analysis)

sided and sidegrooved SENB specimens in the ductile fracture assessments performed with and without residual stresses.

As expected, in general the ductile fracture assessments performed using sidegrooved SENB R curves produced lower values of predicted maximum far field stress than the corresponding assessments based on the plane sided SENB R curves. This is a result of the sidegrooves increasing the constraint in the SENB specimens and consequently reducing the slope of the small scale CTOD R curves. This effect is demonstrated in Figs 5 and 6 which compare the sidegrooved and plane sided CTOD R curves obtained from the small scale SENB specimens taken from panels W17, W18, W19, and W20. It is interesting to note that the difference between the sidegrooved and plane sided CTOD R curves is most pronounced with the through thickness notched specimens, i.e., 50 × 100 mm SENBs. In comparison the plane sided and sidegrooved CTOD R curves obtained from the surface notched specimens (i.e., 50 × 50 mm SENBs) are very similar. This seems to indicate that although the sidegrooves have a major influence on the level of constraint in the 50 × 100 mm SENB specimens, their effect on the 50 × 50 mm SENB specimens is much less pronounced. In the case of the 50 × 50 mm SENB specimens the remaining ligament is more likely to be the controlling parameter since it is only approximately 50 percent of the specimen thickness at the beginning of the test.

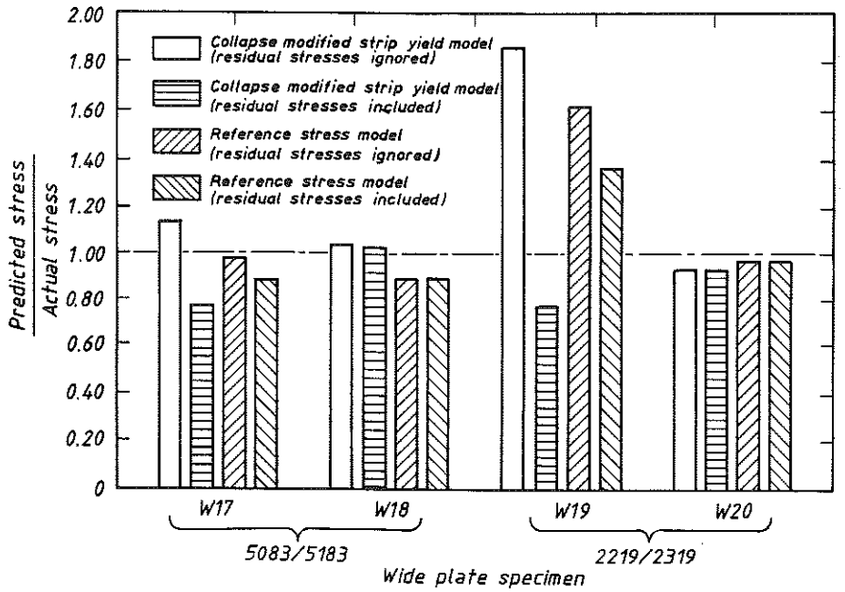

Fig 12 Comparison of tearing instability assessments (CTOD *R* curve obtained from plane sided specimens)

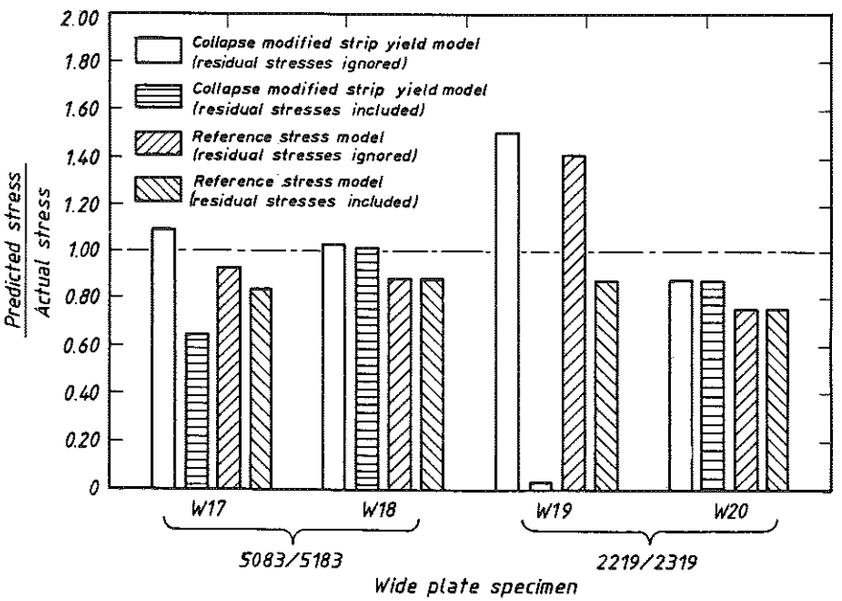

Fig 13 Comparison of tearing instability assessments (CTOD *R* curve obtained from sidegrooved specimens)

The effect of including or ignoring residual stresses in the ductile fracture assessments can be seen by studying Figs 12 and 13, which show the results of the tearing instability analyses performed using plane sided and sidegrooved CTOD *R* curve data, respectively. It should be stressed that the significance of residual stresses with respect to crack growth in the transitional and upper shelf regimes of fracture behaviour is not fully understood. Indeed, it is frequently assumed that residual stresses can be ignored in ductile fracture assessments, since the large applied strains in typical ductile failures will cause the residual stresses to be relaxed. This assumption has merit when ductile instability occurs after net section yield. Whether this is the case when ductile instability occurs before net section yield is open to debate. In this investigation the actual maximum far field stresses in plates W17 and W18 corresponded to net section stresses well above yield. In comparison the maximum load conditions in plates W19 and W20 occurred below net section yield and consequently before plasticity effects became significant. Consequently panels W17 and W18 could be considered as collapse controlled failures whereas panels W19 and W20 were *R* curve controlled failures (i.e., tearing instability).

It is evident from Figs 10 and 11 that failure to include residual stresses in the fracture assessments resulted in several non-conservative estimates of maximum far field stress, particularly in the case of wide plate W19. It is also evident, however, that even if residual stresses are incorporated in the tearing instability analyses, assessments based on plane sided CTOD *R* curve data (as distinct from sidegrooved CTOD *R* curves) can still be non-conservative.

Based on the above observations, it is recommended that ductile fracture assessments of thick section aluminium alloy weldments should be performed using the CTOD reference stress model. Furthermore if the crack under consideration is located in a region where residual stresses are present, then they should be taken into account in the analysis. Finally, to ensure a conservative assessment it is recommended that the crack growth resistance behaviour of the material in which the defect is located should be obtained from full thickness sidegrooved SENB specimens.

Conclusions

The results of a series of welded 50 mm thick aluminium alloy wide plate tests have been compared with predictions obtained using CTOD collapse modified strip yield, and reference stress models. Driving force/*R* curve tearing instability assessments were undertaken. Furthermore, the analyses of the wide plate tests were performed both with and without residual stresses which were measured experimentally. The following points were identified from the tests.

(1) The maximum transverse residual stresses in the weld metals were between 50 and 100 percent of the 0.2 percent proof strength of the weld metals.
(2) The difference between 20 percent sidegrooved and plane sided CTOD *R*

curves in 5183 and 2319 Al weld metals was much more pronounced for B × 2B SENB specimens than for B × B SENB specimens.

(3) Tearing instability analyses using the collapse modified strip yield and reference stress models based on either plane sided CTOD R curve data or performed ignoring residual stresses can be non-conservative.

(4) Provided residual stresses are taken into account, conservative but reasonably accurate, tearing instability assessments were obtained for all wide plate tests using the CTOD reference stress model together with sidegrooved SENB CTOD R curve data. In contrast the collapse modified strip yield model was over conservative using sidegrooved SENB data, but reasonably accurate using plane sided data.

Acknowledgements

This work was funded jointly by Research Members of The Welding Institute and the Minerals and Metals Division of the UK Department of Trade and Industry. The Welding Institute would like to acknowledge Alcoa who supplied the welded aluminium alloy test panels.

References

(1) GORDON, J. R. and GARWOOD, S. J. (1989) A comparison of CTOD ductile instability analyses, *Fracture Mechanics: Twentieth Symposium, ASTM STP 1020*, ASTM, Philadelphia, pp. 410–430.

(2) GARWOOD, S. J. (1988) A crack tip opening displacement (CTOD) method for the analysis of ductile materials, *Fracture Mechanics: Eighteenth Symposium ASTM STP 945*, ASTM, Philadelphia, pp. 957–985.

(3) ANDERSON, T. L. (1985) Elastic–Plastic Fracture Assessments based on CTOD, Welding Institute Research Report 276/1985.

(4) ANDERSON, T. L., LEGGATT, R. H., and GARWOOD, S. J. (1986) The use of CTOD methods in fitness for purpose analyses, *The Crack Tip Opening Displacement in Elastic–Plastic Fracture Mechanics*, (Edited by K.-H. Schwalbe) Springer-Verlag, Berlin, pp. 287–313.

(5) GARWOOD, S. J., GORDON, J. R., WILLOUGHBY, A. A., LEGGATT, R. H., and JUTLA, T. (1988) Crack tip opening displacement (CTOD) methods for fracture assessments: Proposals for revisions to BSI PD6493, The Welding Institute Research Report 371/1988.

(6) TOWERS, O. L. and DAWES, M. G. (1985) Welding Institute Research on the fatigue precracking of fracture toughness specimens, *Elastic–Plastic Fracture Test Methods: Users Experience, ASTM STP 856*, ASTM, Philadelphia, pp. 23–46.

(7) LEGGATT, R. H. (1987) Residual stresses in MIG welded aluminium alloy panels, The Welding Institute Research Report 340/1987.

(8) LEGGATT, R. H. (1983) Residual stresses at girth welds in pipe, Proceeding of Conference, *Welding in Energy Related Projects*, Welding Institute of Canada, Toronto.